Lattice Interferometer for Laser-Cooled Atoms

Mikkel F. Andersen

Atomic Physics Division, National Institute of Standards and Technology, Gaithersburg, Maryland 20899-8424, USA
and Jack Dodd Center for Quantum Technology, Department of Physics, University of Otago, New Zealand

Tycho Sleator

Department of Physics, New York University, 4 Washington Place, New York, New York 10003, USA

We demonstrate an atom interferometer in which atoms are laser cooled into a 1D optical lattice, suddenly released, and later subjected to a pulsed optical lattice. For short pulses, a simple analytical theory predicts the signal. We investigate both short and longer pulses where the analytical theory fails. Longer pulses yield higher precision and larger signals, and we observe a coherent signal at times that can differ significantly from the expected echo time. The interferometer has potential for precision measurements of $\hbar/m_A$, and can probe the dynamics of atoms in an optical lattice.

Matter wave interference has intrigued scientists since the early days of quantum mechanics. Still today, its fundamental nature is a field of intense research, and beautiful demonstrations and investigations shedding light on this phenomenon have been performed in the past decade. These include interference of "large" objects and of biomolecules [1], interference of independently prepared particles [2], and the origin of quantum mechanical complementarity [3]. Advances in microfabrication techniques and the development of laser cooling and trapping for neutral atoms have opened up many new possibilities for constructing atom interferometers [4]. Besides testing the fundamental nature of matter wave interference, atom interferometers play an essential role in many high precision measurements, where the accurate determination of fundamental constants, such as the fine structure constant α and the Newtonian constant of gravity, by several independent means, tests the borders of our understanding [5–7]. Moreover, precise measurements of quantities such as the local gravitational field hold promise for technological advances in navigation and mineral exploration [8].

In this Letter, we demonstrate a new type of echo-interferometer [5,9–14]. It is simple and uses atoms initially laser cooled and loaded into a one-dimensional (1D) optical-lattice potential, released, and later exposed to a pulse of the lattice potential. This single pulse interferometer enhances the signal by more than a factor of 4 compared to the two pulse interferometer in Ref. [11]. It can be used for a precision measurement of the recoil frequency $\omega_k = \hbar k^2/(2m_A)$, where m_A is the atomic mass and k the wave vector of a laser field. This quantity is of great interest for testing fundamental theories [5,7,12]. Our interferometer shares the robustness against vibrations, accelerations, rotations, magnetic field gradients, and differences of ac Stark shifts between internal levels of those demonstrated in [11,12], without the systematic errors due to interactions

between the atoms the use of a Bose-Einstein condensate (BEC) can inflict [12].

We investigate how our interferometer performs when the optical-lattice pulse violates the "short" pulse or Raman-Nath limit (a regime not previously investigated in related interferometers), and find that a moderate violation of this limit can enhance the performance of the interferometer. We show that the interferometer reveals information on the quantum dynamics of atoms in an optical-lattice potential, and thereby that it holds promise for use in the study of driven 1D systems [15]. Furthermore, we find that for specific pulse lengths, a coherent signal can occur at times that differ from the expected echo time by as much as 10 times the coherence time expected from the initial momentum spread of the atoms.

Figure 1 shows a time line of our experiment, which uses a vapor cell magneto optical trap (MOT) for ^{85}Rb atoms loaded for 40 ms. An optical molasses stage of 7 ms further cools the atoms and loads them into the optical lattice, which is formed by two vertically polarized horizontally propagating laser beams with wave vectors $\mathbf{k}_1$ and $\mathbf{k}_2$, an angle of 162° between them, and detuned 395 MHz above
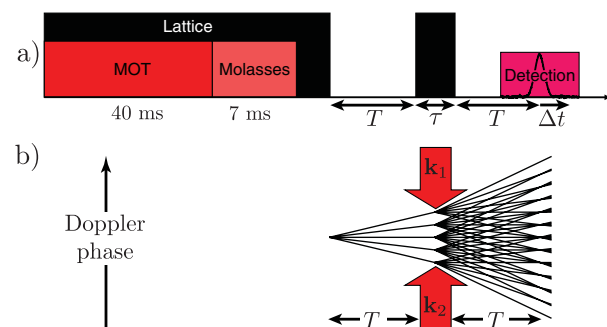

FIG. 1 (color). (a) Time line of the experimental cycle. (b) Doppler phase diagram for atoms released from optical lattice.

the $|5S_{1/2}, F = 3\rangle$ to $|5P_{3/2}, F' = 4\rangle$ transition. The lattice laser beams are clipped Gaussian beams with a diameter larger than the MOT cloud, so all the atoms in the MOT are loaded into the lattice. After the molasses stage, which cools the atoms to ~ 36 μK, the repump laser remains on for 100 μs to prepare the atoms in the $F = 3$ ground state. Acusto-optic modulators control the optical-lattice beams. At time $t = 0$ (10 μs after the turnoff of the repump light), we abruptly (in ~ 20 ns) turn off the optical lattice. After leaving the atoms in darkness for a time T, we pulse the optical lattice on for a short time τ. Later, we detect the amplitude of atomic density modulations with period $2\pi/q$ with $\mathbf{q} = \mathbf{k}_1 - \mathbf{k}_2$ by applying a weak off-resonant optical field along direction $\mathbf{k}_1$ and measuring the amplitude of the field Bragg scattered off the atomic density modulation along the direction $\mathbf{k}_2$ using a heterodyne technique [11].

To calculate the expected signal, we assume that the atoms are in thermal equilibrium in the optical lattice, and localized to narrow regions near the potential minima, so they form a periodic density distribution and effectively experience a harmonic oscillator potential. Since the temperature of the atoms is ~ 36 μK, their thermal de Broglie wave coherence length is much shorter than the period of the optical lattice. Under these conditions, it can be shown that the atoms closely approximate an incoherent mixture of states identical to the ones obtained by an atomic plane wave of momentum $\mathbf{q}_0$ impinging on a periodic array of Gaussian transmission functions with width σ (the width of the atomic density distribution in a single minimum in the lattice) and period $2\pi/q$,

$$\psi_{\mathbf{q}_0}(\mathbf{x}, 0) = \sum_{n_1=-\infty}^{\infty} e^{-n_1^2(q\sigma)^2} e^{i(\mathbf{q}_0 + n_1\mathbf{q})\cdot\mathbf{x}}, \qquad (1)$$

where each state $\psi_{\mathbf{q}_0}$ contributes with a weight given by the momentum ($\hbar\mathbf{q}_0$) distribution of a gas of atoms in thermal equilibrium. The experimental signal can be computed by first calculating the signal resulting from the system initially in state $\psi_{\mathbf{q}_0}(\mathbf{x}, 0)$ and then summing this signal over the distribution of $\mathbf{q}_0$.

After the lattice is turned off at $t = 0$, each plane wave, $\exp[i(\mathbf{q}_0 + n\mathbf{q})\cdot\mathbf{x}]$ in Eq. (1) acquires a phase $\phi = (\omega_{q_0} + n_1^2\omega_q + n_1\mathbf{q}\cdot\mathbf{v}_0)t$, where $\omega_q = \hbar q^2/2m$ is the (two-photon) recoil frequency and $n_1\mathbf{q}\cdot\mathbf{v}_0 t$ is the Doppler phase, which is proportional to the initial atomic velocity $\mathbf{v}_0 = \hbar\mathbf{q}_0/m$. The optical-lattice pulse, turned on at time $t = T$, diffracts each plane wave into a set of plane waves with wave vectors differing by integer multiples of $\mathbf{q}$ [16]. If τ is so short that atomic motion can be neglected during the pulse (Raman-Nath condition), then no Doppler phase evolution occurs during this time. Figure 1(b) shows a diagram of the Doppler phase evolution of various amplitudes as a function of time in our interferometer. Crossing lines in the diagram occur at times when different momentum states have the same Doppler phase, and atomic fringe patterns are produced at these times. In particular, fringe patterns with period $2\pi/q$ are produced

close to times $t_N = (N + 1)T$ for positive integer N (t_N are called the echo-times). A detailed calculation similar to the one in Ref. [11], which assumes that the interaction during the pulse is given by $H = \frac{1}{2}V_0\cos(\mathbf{q}\cdot\mathbf{x})$, gives a signal proportional to

$$S(\Delta t) = e^{-(qu\Delta t/2)^2}$$
$$\times e^{-(1/2)N^2(q\sigma)^2} J_{N+1}[2\theta\sin(N\omega_q T + \omega_q\Delta t)], \quad (2)$$

where $u = \sqrt{2k_B\mathcal{T}/m_A}$, k_B Boltzmann's constant, $\mathcal{T}$ the temperature of the atoms, $\Delta t \equiv t - t_N$, and $\theta = \tau V_0/(2\hbar)$ is a pulse area.

Figure 2 shows the signal obtained at around $T = 81$ μs with a short pulse of duration $\tau = 350$ ns. All data shown correspond to the fundamental echo $N = 1$. Our temperature estimate is found by fitting Eq. (2) to the data. The signals shown in Fig. 2 are the largest we could obtain in the short pulse limit with the laser power and detuning we use. In contrast to the signal obtained from the interferometer in [11] (also shown in Fig. 2 for a similar number of atoms), our interferometer signal reaches a maximum at the echo time ($\Delta t = 0$) and with a maximal signal size more than a factor of 4 larger than that of Ref. [11], demonstrating an improved signal-to-noise ratio and higher contrast of the atomic density modulation. We ascribe this to the fact that in our interferometer the signal is an echo of a density modulation of the atoms, whereas in Ref. [11] it is a velocity (or phase) modulation, that with time evolves into a density modulation, but also partially dephases due to the thermal velocity spread of the atoms. By laser cooling the atoms into the optical lattice, we avoid
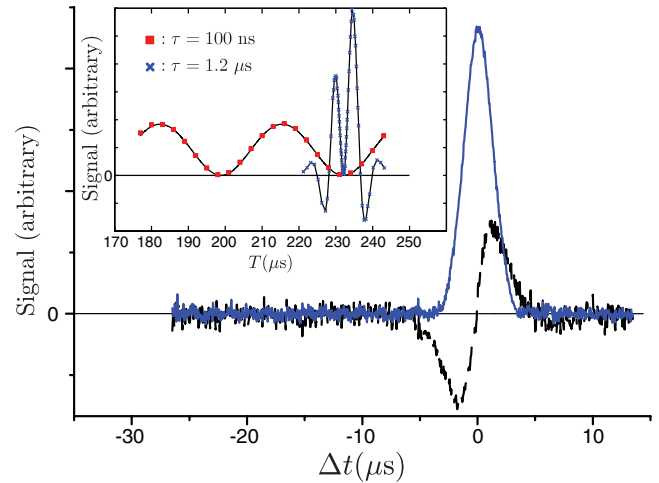

FIG. 2 (color). Solid blue curve: Signal from lattice interferometer for $\tau = 350$ ns and $T = 81$ μs. Dashed black curve: Maximal signal we could obtain from the interferometer described in [11]. Inset: Peak signal as a function of pulse separation T for small area pulses $\tau = 100$ ns (red squares). Peak signal theoretically expected from Eq. (2) (corresponding solid curve). Blue crosses connected by a black line: The measured peak signal for $\tau = 1.2$ μs, too long for the Raman-Nath condition. The longer pulse yields sharper features in the signal.

the large loss of atoms, associated with using an optical
mask [13] (the atom optics analog of an absorption grating
in light optics) for generation of the atomic density modu-
lation. Note that the revival of the density modulation
shows that the atomic state continues to carry the informa-
tion of its lattice preparation, despite its density distribu-
tion shortly after release being indistinguishable from a
thermal cloud. This is analogous to experiments reported in
Refs. [17,18] where it was shown that preparation in an
optical lattice is revealed in the noise correlation after time
of flight.

Equation (2) also shows that the peak signal at the echo
time varies periodically as a function of T with period
given by the Talbot time $T_T = 2\pi/\omega_q$. Our interferometer
can therefore be used to measure the Talbot time (or
equivalently, the recoil frequency), which together with
other well-known constants constitutes a measurement of
the fine structure constant α [5,7,12]. The inset of Fig. 2
shows the analytical prediction [Eq. (2)] together with the
experimental measurements of the peak signal as a func-
tion of T for a pulse length of 100 ns. In the analytical
prediction, we use $V_0/h = 2.0$ MHz determined in a sepa-
rate measurement of the τ that yields the first maximum in
the signal for $T = 81$ μs. The overall amplitude was ad-
justed to fit the data. By comparing the size of the echo
signal for $N = 1, 2,$ and 3, we can use Eq. (2) to extract the
degree of localization σ of the atoms in the lattice, and find
that $\sigma = 55$ nm. This could be reduced by using a BEC
released from an optical lattice.

Sharp features in the interferometric signal as a function
of T (or equivalently higher frequency components in the
signal) improves the precision with which we can deter-
mine the Talbot time and recoil frequency [19]. From
Eq. (2), we see that if we increase θ, more oscillations
and sharper features occur in each period when T is
scanned, thereby improving the sensitivity of the interfer-
ometer. V_0 and thereby θ can be increased by increasing
the power in the lattice beams, but the above results are
obtained using the maximum laser power we have avail-
able. Increasing τ will also increase θ, but this will even-
tually lead to a break down of the Raman-Nath condition,
and thereby the validity of Eq. (2). When the Raman-Nath
condition is violated, the signal is still periodic in T with
period T_T independent of pulse duration. Thus, the recoil
frequency can be determined simply from this period. We
therefore investigate what happens when the pulse length is
increased beyond the Raman-Nath limit. In Fig. 3, we
present the echo signal as a function of T and Δt for
different pulse durations τ. For $\tau = 1.2$ μs [Fig. 3(c)],
we see a clear deviation from the results predicted by
Eq. (2), namely, that the signal vanishes for Ts around
$(n + 1/2)T_T/2$ with n an integer, and that the signal is
asymmetric around $nT_T/2$. However, the narrow "dark"
fringe around $nT_T/2$ persists, enabling an accurate deter-
mination of T_T. Our experimental observation that the
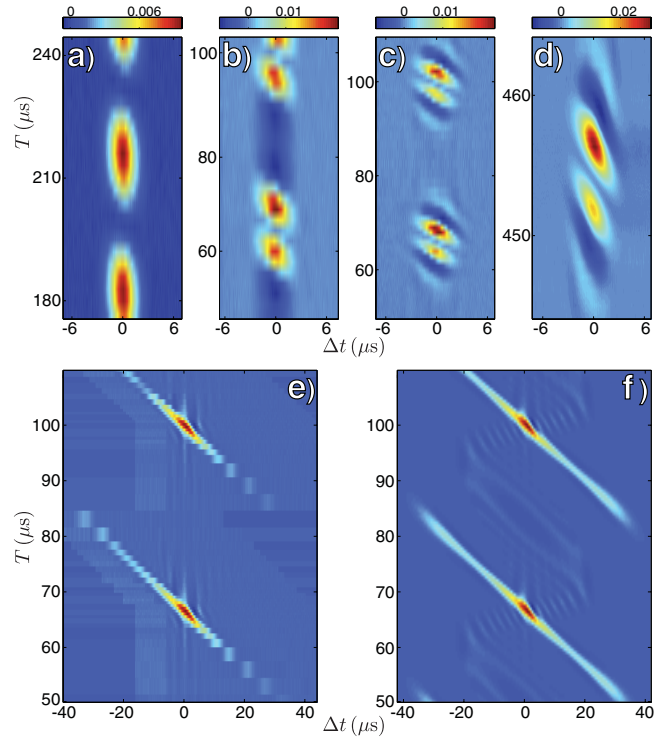sharpest features of the echo signal are found for pulse

FIG. 3 (color). Echo signal (color coded) as a function of Δt
and time of the pulse T (the echo time is $t_1 = 2T + \tau$). The inset
in Fig. 2 is a vertical cross-section at the echo time ($\Delta t = 0$) and
the main data in Fig. 2 a horizontal cross-section of the data in
this figure. (a), (b), and (c): Experimental data for pulse dura-
tions $\tau = 100$ ns, 600 ns, and 1.2 μs. For $\tau = 1.2$ μs, the signal
vanishes for all T around 80 μs. (d) High resolution experimen-
tal data $\tau = 1.2$ μs. (e) Experimental data for $\tau = 3.5$ μs.
Features as a function of T are no longer as sharp as for $\tau =$
1.2 μs. We observe a coherent signal for times that differ highly
from the echo time. (f) Numerical calculation of the expected
signal for the parameters of (e).

durations between 1 μs and 2 μs is not surprising, since
the optical lattice imparts maximum momentum into the
atoms for durations around $\tau \sim 1/4\tau_{osc}$ (τ_{osc} is the oscil-
lation period of an atom close to a potential minimum). We
use the sharp features described above to determine the
Talbot time by taking data with high resolution in T for
$\tau = 1.2$ μs around $T = 65$ μs and around $T = 455$ μs
[see Fig. 3(d)]; that is, differing in T by about 6 Talbot
times. From this, we obtain a value of $h/m_{Rb} = 4.6997 \times$
$10^{-9} \pm 0.0003 \times 10^{-9}$ m^2/s^2 [20], with m_{Rb} the mass of a
^{85}Rb atom, in agreement with the value of $h/m_{Rb} =$
4.6994×10^{-9} m^2/s^2 deduced from [21]. Our "large"
uncertainty arises from the determination of the angle
between the beams, a problem that can be overcome by
using counterpropagating beams and coupling between
optical fibers [7,14].

For $\tau = 3.5$ μs [see Fig. 3(e)], we observe the interest-
ing phenomenon that a coherent signal for certain values of
T is observed for times that differ from the echo time
($2T + \tau$) by as much as 40 μs. This is more than 10 times
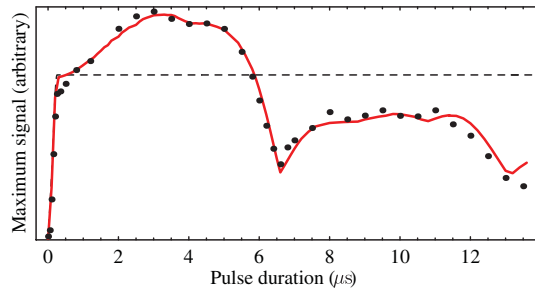the decoherence time of few μs expected from the initial

FIG. 4 (color). Maximum signal as a function of pulse duration. Dots are the data, and the solid curve is a numerical calculation multiplied by an exponential decay to accommodate for decoherence due to photon scattering. Dashed line is the maximum signal expected from Eq. (2) and does not show oscillations. We see that violating the Raman-Nath condition can increase the contrast of the atomic density modulation.

thermal spread of atoms. The nature of the signal also seems to indicate its occurrence is not due to long coherence times, but rather because the dynamics of the atoms during the lattice pulse enables a coherent rephasing at this time. We note that this phenomenon occurs for pulse durations τ around $\frac{1}{2}\tau_{\mathrm{osc}}$. In Fig. 3(f), we show a 1D numerical calculation of the expected signal for the same parameters as the experimental results in Fig. 3(e) (no photon scattering is included in the calculation).

To further investigate the dynamics of the atoms in the optical lattice, we measured the maximum signal size for a given τ by scanning T. In Fig. 4, we plot this maximum signal as a function of τ. We observe that violating the Raman-Nath limit can improve the contrast of the atomic density modulation since pulse lengths from 1 to 5 μs yields a larger signal than predicted by Eq. (2) (also shown in Fig. 4). In contrast to the prediction of Eq. (2), the signal shows damped oscillations with a period of around 6.6 μs. This period is consistent with τ_{osc} reflecting a partial revival of the initial state at this time. This effect has been observed previously using a BEC in an optical lattice [16], and the fact that it easily is seen in our data indicates that our interferometer can be used as a sensitive probe of the quantum dynamics in diffracting structures, including classical chaotic systems such as the δ-kicked rotor [15]. In Fig. 4, we also show a numerical calculation of the expected maximum signal as a function of τ. To account for decay of coherence due to photon scattering in the optical lattice, the numerical calculation shown in Fig. 4 has been multiplied by an exponential decay as function of τ where the decay rate of 3.5×10^4 s^{-1} is found by fitting to the data. This decay rate is smaller than the average photon scattering rate of 9×10^4 s^{-1} calculated from our measured value of V_0 and the detuning of the light. The effect of photon scattering on coherence will be the topic of future investigations.

In summary, we have demonstrated a simple atom interferometer that uses atoms, laser cooled into an optical lattice, followed by an optical-lattice pulse. Our technique is capable of producing atomic density modulations with a contrast significantly higher than the interferometer in Ref. [11]. This increases the signal-to-noise ratio of the interferometric signal, and could also be of interest in atomic lithography. In this field, our technique has the advantage over the previously demonstrated optical mask technique [13] in that it generates an spatial atomic density modulation, and not a spatial internal state modulation. We investigated how the interferometer performs when the pulse violates the Raman-Nath condition and found that a moderate violation can improve the sensitivity and increase the contrast of the atomic density modulation. For specific pulse lengths in the long-pulse regime, we observe a coherent signal at times that differ greatly from the echo time. We showed that the interferometric signal can be used as a sensitive probe of the dynamics of the atoms in the optical lattice. Our technique reveals the degree of localization of atoms in an optical lattice, and may therefore be employed in the study of superfluid to Mott-insulator quantum phase transition of BECs in optical lattices [18,22].

[1] L. Hackermuller *et al.*, Nature (London) **427**, 711 (2004);
     L. Hackermuller *et al.*, Phys. Rev. Lett. **91**, 090408 (2003).
[2] M. R. Andrews *et al.*, Science **275**, 637 (1997).
[3] S. Durr, T. Nonn, and G. Rempe, Nature (London) **395**, 33 (1998).
[4] A. Cronin, J. Schmiedmayer, and D. Pritchard, arXiv:0712.3703 [Rev. Mod. Phys. (to be published)].
[5] D. S. Weiss, B. C. Young, and S. Chu, Phys. Rev. Lett. **70**, 2706 (1993).
[6] J. B. Fixler *et al.*, Science **315**, 74 (2007).
[7] P Cladé *et al.*, Phys. Rev. Lett. **96**, 033001 (2006).
[8] J. M. McGuirk *et al.*, Phys. Rev. A **65**, 033608 (2002).
[9] D. W. Keith *et al.*, Phys. Rev. Lett. **66**, 2693 (1991).
[10] M. Weitz, T. Heupel, and T. W. Hänsch, Phys. Rev. Lett. **77**, 2356 (1996).
[11] S. B. Cahn *et al.*, Phys. Rev. Lett. **79**, 784 (1997).
[12] S. Gupta *et al.*, Phys. Rev. Lett. **89**, 140401 (2002).
[13] A. Turlapov, A. Tonyushkin, and T. Sleator, Phys. Rev. A **71**, 043612 (2005).
[14] H. Müller *et al.*, Phys. Rev. Lett. **100**, 180405 (2008).
[15] M. G. Raizen, Adv. At. Mol. Opt. Phys. **41**, 43 (1999).
[16] Y. B. Ovchinnikov *et al.*, Phys. Rev. Lett. **83**, 284 (1999).
[17] S. Fölling *et al.*, Nature (London) **434**, 481 (2005).
[18] I. B. Spielman, W. D. Phillips, and J. V. Porto, Phys. Rev. Lett. **98**, 080404 (2007).
[19] F. S. Cataliotti *et al.*, Phys. Rev. Lett. **87**, 113601 (2001).
[20] The uncertainties are 1 standard deviation combined systematic and statistical.
[21] G. Audi, A. H. Wapstra, and C. Thibault, Nucl. Phys. A **729**, 337 (2003).
[22] M. Greiner *et al.*, Nature (London) **415**, 39 (2002).